

Dynamics of Vortex Nucleation in Nanomagnets with Broken Symmetry

Jaroslav Tóbiš,^{1,*} Vladimír Cambel,¹ and Goran Karapetrov^{1,2}

¹*Institute of Electrical Engineering, Slovak Academy of Sciences,
Dúbravská cesta 9, SK-841 04 Bratislava, Slovakia*

²*Department of Physics, Drexel University, 3141 Chestnut Street, Philadelphia, Pennsylvania 19104, USA*

(Dated: November 10, 2018)

We investigate fundamental processes that govern dynamics of vortex nucleation in sub-100 nm mesoscopic magnets. We focus on a structure with broken symmetry - Pacman-like nanomagnet shape - in which we study micromagnetic behavior both by means of a simple model and numerically. We show that it is possible to establish desired vortex chirality and the polarity of vortex core by applying only quasi-static in-plane magnetic field along specific directions. We identify the modes of vortex nucleation that are very robust against external magnetic field noise. These vortex nucleation modes are common among wide range of sub-100 nm magnets with broken rotational symmetry.

PACS numbers: 75.75-c, 75.60.Jk, 75.78.Cd

Confinement leads to fundamental changes in physical behavior of materials due to increased role of the surface. In mesoscopic magnetic materials such changes in the energy landscape could lead to novel magnetic spin configurations such as vortices. Equilibrium properties of these new topological states are governed by both the properties of the magnetic material and the geometry of the object. On the other hand, confinement also leads to distinct dynamic behavior of the new topological states, since the available energy levels are very much limited. The transition probabilities between different states can thus be controlled by careful engineering of the geometry of the mesoscopic object. Here we show that by tailoring the geometry of the mesoscopic magnet one can produce deterministic dynamic switching between well defined degenerate topological states using only in-plane magnetic pulses. We present a simple model that explains the mechanism of the vortex nucleation and origin of robustness of the vortex polarization. Confirmation of the model is accomplished by using numerical simulations.

Controlled manipulation of magnetic domains in ferromagnet nanostructures have recently opened opportunities for novel fast, high-density, and low-power memories with novel architectures¹⁻³. Any perspective magnetic memory architecture, such as sub-micron non-volatile magnetic memory, has to have (1) a well-defined switching field used to set the memory bits, and (2) a reproducible switching behavior using simple sequence of external magnetic field pulses. Therefore, the dynamics of the switching between different ground states has to be understood in detail.

Recent advances in fabrication technology at nanoscale have enabled studies of magnetic systems that are well defined in all three dimensions on a nanometer length scale (< 100 nm)^{4,5}. The size reduction of nanomagnets leads to novel spin topological states such as vortex state, C- state, S-state, flower state, etc.⁶, and to simplified transitions between these states in external magnetic field. The transition between ground states in such nanomagnets is of fundamental importance⁷. It

is governed by competition between the magneto-static energy and exchange energy, and it is influenced by the magnetic material used and by the choice of the nanomagnet shape. For example, the magnetization of disks in zero field can be oriented in-plane, out-of-plane, or vortex state can be created, depending on the disk diameter and thickness^{4,8}. In the disk the flux-closure magnetic state reduces the long range stray fields, i.e. reduces the magnetostatic interaction between neighboring disks. Therefore, such disk magnetic systems have a potential for high-density magnetic storage elements, with bits represented by chirality and polarity of a basic vortex state.

In sub-micron sized disks four possible states have to be controlled. It was shown experimentally that in the nanomagnets with broken rotational symmetry, chirality can be controlled easily by in-plane field of selected direction⁹⁻¹². At the same time the polarity of the vortex core, which represents the second bit, can be controlled by an out-of-plane magnetic field¹², spin-polarized current¹³, high-frequency in-plane magnetic field¹⁴, or by an in-plane magnetic pulse of precisely defined amplitude and duration¹⁵.

In our previous work we have proposed a new prospective shape of a nanomagnet with broken symmetry which permits control of chirality and polarity bits by the application of the in-plane field only¹⁶. In this paper we analyze the mechanisms that establish specific chirality and polarity values in such Pacman-like (PL) nanomagnet by taking a closer look at energies and dynamics that govern the switching processes. We show that the polarity and the chirality of the vortex core nucleated in the decreasing in-plane magnetic field is implicitly defined by the direction of the magnetic field with respect to missing sector of the PL nanomagnet.

We consider a magnetic dot of cylindrical shape. To construct a PL structure it is necessary to remove an outer sector that is 45° wide, and has $1/3$ of the disk radius (see Fig. 1). Due to symmetry analysis that will be presented later, we choose the orientation of x, z axes such, that they define mirror symmetry plane σ_y , which leaves PL object invariant. Another symmetry operation

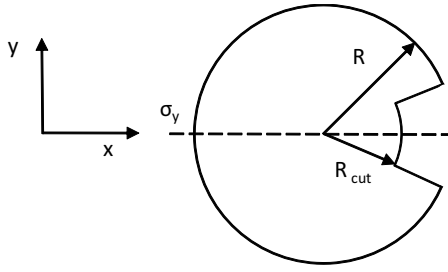


FIG. 1. Geometry of Pacman-like nanomagnet. The structure is symmetric with respect to reflection plane σ_y .

is mirroring through the plane x, y noted in following text by σ_z .

First, we define polarity $\vec{\pi}[\vec{f}]$ and chirality $\vec{\chi}[\vec{f}]$ vectors as functionals of an arbitrary vector field \vec{f} :

$$\begin{aligned}\vec{\pi}[\vec{f}] &= \frac{1}{\Omega} \int \vec{f}(\vec{r}) d\Omega \\ \vec{\chi}[\vec{f}] &= \int \vec{r} \times (\vec{f}(\vec{r}) - \vec{\pi}) d\Omega\end{aligned}\quad (1)$$

Polarity is just simple average value of the field, while chirality resembles the definition of momentum of quantity \vec{f} in classical mechanics. Subtraction of polarity in the expression for chirality is necessary due to chirality invariance with respect to the origin coordinate system choice. Mostly we are interested in z component of polarity and chirality. Integration domain Ω is over the volume of the PL nanomagnet.

Let's consider that the nanomagnet is placed in a strong in-plane magnetic field that has an angle φ with the x -axis. To emulate magnetic response by the missing sector, we can consider the PL nanomagnet as a superposition of a full disk and a set of microscopic magnetic moments in a removed sector. These additional moments have to have the same value and to be oriented in opposite direction to the magnetic moments in the disk (Fig. 2). In the first approximation all microscopic moments are parallel. Neglecting higher than dipolar moments, missing sector behaves as a dipole with a moment \vec{m}_{cut} positioned in the center of mass of the sector \vec{r}_T :

$$\vec{m}_{\text{cut}} = - \int \vec{M} d\Omega' \quad \vec{r}_T = \frac{1}{\Omega'} \int \vec{r} d\Omega'. \quad (2)$$

Minus sign reflects that dipoles of opposite orientation have to be added in order to eliminate dipoles in the missing sector (see Fig. 2). The integration is over the volume of the missing sector Ω' .

To calculate the magnetic field of PL nanomagnet consider first the full disk. In magnetic fields exceeding the saturation field the magnetic polarization \vec{M} is parallel to the direction of the applied field \vec{H}_{ext} throughout the disk volume. Internal magnetic field \vec{H} is also uniformly oriented in parallel with \vec{M} . As small piece of material is removed, all the fields change slightly. To correct

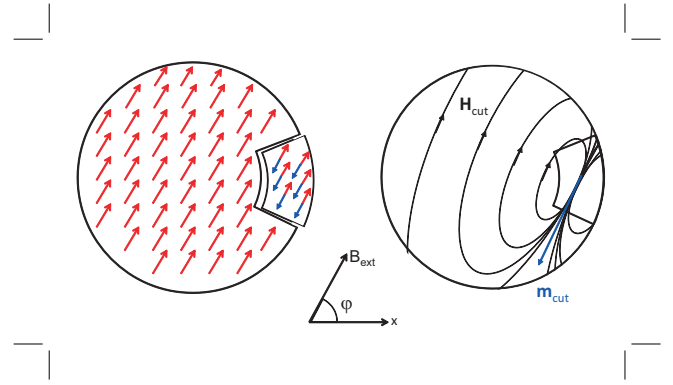


FIG. 2. (a) The magnetization of the Pacman-like nanomagnet is a superposition of the uniform magnetization of a full disk (red arrows) and the magnetization of the missing sector that is equal and opposite to the one of the full disk. (b) The sum of the compensation moments in the sector creates a dipole m_{cut} which asymmetrically interacts with the local magnetization in the nanomagnet.

the internal magnetic field, the field of magnetic moment \vec{m}_{cut} given by equation (2) has to be added to the originally homogeneous internal field of the full disk. The removed part thus creates a dipole which induces magnetic field with non-zero chirality $\chi[\vec{H}]$, if $\varphi \neq 0^\circ, 180^\circ$. Since dipoles partially follow the field orientation, the non-zero chirality of \vec{M} is expected.

Next, we explain qualitatively the mechanism which determines vortex core polarity. Taking into consideration magneto-statics only, the state with positive polarity $\pi[\vec{M}]$ is energetically equivalent to the state with negative polarity $-\pi[\vec{M}]$, if no external field in z direction is applied. That can be easily seen by writing the total energy functional:

$$\begin{aligned}E &= \frac{\mu_0}{4\pi} \int \int \left(\frac{\vec{M} \cdot \vec{M}'}{|\vec{r} - \vec{r}'|^3} - \frac{3\vec{M} \cdot (\vec{r} - \vec{r}') \vec{M}' \cdot (\vec{r} - \vec{r}')}{|\vec{r} - \vec{r}'|^5} \right) d\Omega d\Omega' \\ &+ A \int (\nabla \vec{M})^2 d\Omega - \int \vec{H}_{\text{ext}} \cdot \vec{M} d\Omega\end{aligned}\quad (3)$$

Changing the sign of M_z does not change first two integrals of the equation (3), since these two parts of the energy functional are quadratic in M_z and its derivative, respectively. The only linear part in M_z is in the third integral. But a change of sign of M_z would not influence the total energy, because \vec{H}_{ext} has no z component. Integration domain Ω is not changed by reversing z , because symmetry operation σ_z - reflection from the plane xy transforms PL nanomagnet to itself.

The final state of vortex core polarization is determined by magnetization dynamics. Time evolution of magnetization is described by phenomenological Landau-Lifshitz-Gilbert (LLG) equation:

$$\frac{\partial \vec{M}}{\partial t} = -\gamma \vec{M} \times \vec{H}_{\text{eff}} + \alpha \left(\vec{M} \times \frac{\partial \vec{M}}{\partial t} \right) \quad (4)$$

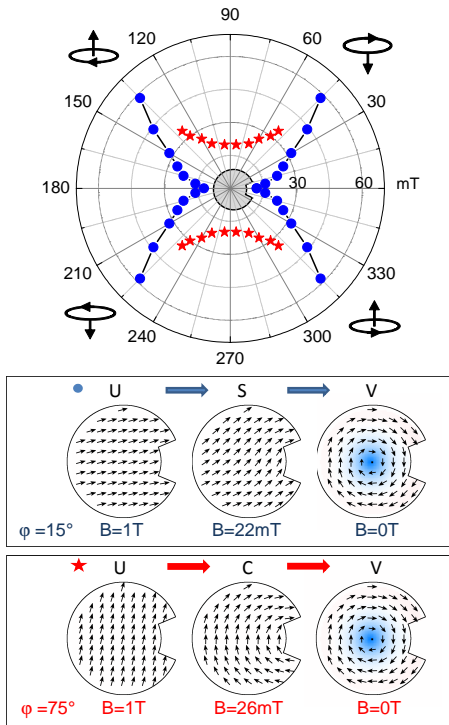


FIG. 3. Angular dependence of the vortex nucleation process. Top: angular dependence of vortex nucleation field. Direction of the nucleated vortex polarity and chirality are also indicated for each quadrant. Bottom: two different processes of vortex nucleation depending on initial magnetization direction with respect to PL's symmetry plane ($\varphi = 15^\circ$ and $\varphi = 75^\circ$): from uniform magnetization state the magnetization transitions to S-shape (dots) or C-shape (stars) configurations and equilibrates to a vortex state with specific polarity and chirality.

Here we show that this equation itself contains polarity symmetry breaking mechanism. First, we apply strong external in-plane field in direction that has an angle φ with the x -axis (Fig.2). Then we slowly (adiabatically) decrease the external field amplitude to the level that is just above the vortex nucleation field. By adiabatic field change we mean that the change of the external field with time is so slow, that the energy dissipation keeps the system very close to the local minimum at all times. Then $\frac{\partial \vec{M}}{\partial t} \approx 0$ everywhere. Any dynamics means also dissipation of energy due to term that is proportional to α in equation (4). Therefore, at local minima we also have $\vec{H}_{\text{eff}} \approx 0$, otherwise it is not possible to satisfy equation (4) with vanishing left side. Now, having \vec{H}_{ext} just above nucleation field, we decrease the external field by a small value $\Delta \vec{H}$. To first approximation the effective field is $\vec{H}_{\text{eff}} = \Delta \vec{H}$. When looking at the dynamics of

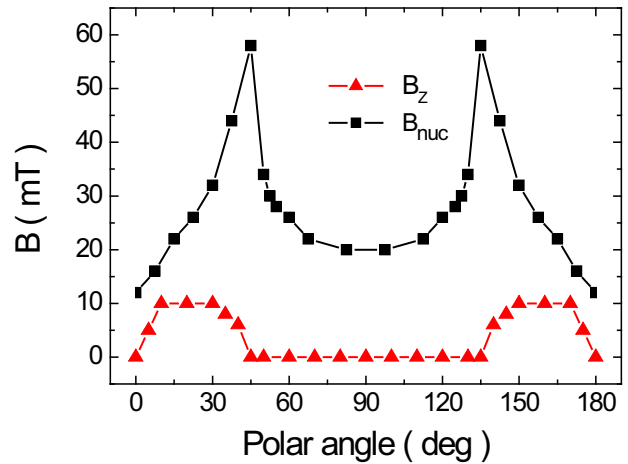


FIG. 4. Angular dependence of the in-plane vortex nucleation field B_{nuc} and threshold out-of-plane field B_z necessary to reverse the polarity of the entering vortex.

local magnetic moments shortly after the external field is decreased, we can neglect the damping term in the LLG equation, since $\alpha \ll 1$. The dynamics of M_z is then governed by the equation

$$\frac{\partial M_z}{\partial t} = -\gamma (M_x \Delta H_y - M_y \Delta H_x). \quad (5)$$

The right-hand side of the equation (5) is not zero locally, nor it is in average, due to asymmetry of the PL nanomagnet with respect to the direction of the applied field (if $\varphi \neq 0^\circ, 180^\circ$). If the actual value of the external field is lower than the nucleation field, the non-zero polarity of the nanomagnet will emerge. Paths towards two equivalent minima characterized by $\pm M_z$ are energetically equivalent, but change of external field with time is biasing the time evolution of magnetization towards configuration given by eq. (5).

Confirmation of the above model approximation can be obtained by numerical simulations. We have performed numerical simulations of PL nanomagnet using OOMMF software package¹⁷. Parameters used in the simulation are: outer radius $R = 35$ nm, thickness (in z -direction - not shown) $h = 40$ nm. Material used in the calculations was Permalloy $\text{Ni}_{80}\text{Fe}_{20}$ (Py), with following material parameters: exchange constant $A = 13 \times 10^{-12}$ J/m and saturated magnetization $M_s = 8.6 \times 10^5$ A/m.

In Figure 3 we show the dependence of the nucleation-field amplitude on the applied field direction. The nucleation field is defined as the applied magnetic field at which the non-zero z component of the magnetization polarity $\pi(\vec{M})$ appears. External field is adiabatically decreasing from 150 mT to zero in selected direction. By adiabatic change we mean repeated process of decreasing field by 2 mT step, followed by full system relaxation.

We would like to note the symmetry properties of PL nanomagnet. In Fig. 3(top) each quadrant corresponds

to a vortex ground state of the nanomagnet with specific chirality and polarity shown in corresponding corners. The nanomagnet relaxes into that remanent state from a uniform magnetization along an angle within the specific quadrant. As can be seen in Fig.3, angular dependence of the nucleation field can be reconstructed from the dependence for $\varphi \in [0; \frac{\pi}{2}]$ by inversion and reflection through xz plane σ_y . Inversion symmetry of the graph shown in Fig.3 is the consequence of the time-reversal symmetry. The reflection symmetry with respect to xz plane shown in Fig.3 is related to reflection from σ_y - geometrical operation that transforms PL nanomagnet to itself.

The simulation results show the existence of *two distinct vortex core nucleation regimes* (Fig.3 (bottom)). For large angles ($\varphi \in [50^\circ; 90^\circ]$) - vortex nucleates from C-state magnetization pattern. This form of nucleation is not robust in the sense that even small out-of-plane field $B_z \simeq 1\text{mT}$ is sufficient to alter the resulting polarity of the nucleated vortex along the direction of applied field B_z . Instead, for small angles ($\varphi \in [0^\circ; 48^\circ]$) - the vortex nucleation path is different. Just above the vortex nucleation field, the magnetization of PL nanomagnet forms an S-state. This configuration consists of two regions with opposite signs of the curvature of field lines¹⁸. Meanwhile, there is only one curvature of field lines just below the vortex nucleation field. The process of vortex core nucleation in this case involves *reversal of magnetic moments* in a part of the nanomagnet. This reversal process proceeds through an out-of-plane motion of the local magnetic moments, resulting in robust vortex core polarization despite the presence of small external fields in z direction. In figure 4 we show the angular dependence of the maximum external field B_z for which the PL nanomagnet is able to sustain nucleation of vortex polarity opposite to the direction of applied external field.

The C and S-shapes of magnetization can be explained by the position of perturbing dipole \vec{m}_{cut} . As can be seen from the Fig.2, PL nanomagnet is divided into two domains with opposite sign of magnetic field circulation generated by \vec{m}_{cut} . The size of this two domains are

determined by orientation of \vec{m}_{cut} . However, exchange interaction tends to align local moments in parallel, thus there exists a critical angle (around 48° in our geometry), beyond which the region with minor curvature does not exist. Detailed energy balance between exchange and cavity (sector) demagnetization determines the scenario of vortex nucleation and its eventual robustness with respect to external perturbation.

To summarize, in this work we provide simple arguments that elucidate the origin of driving mechanisms for nucleation of magnetic vortex with controlled chirality and polarity. We have also found the regime of PL nanomagnet operation in which the final vortex state is independent on weak disturbing external field. This is a promising finding to consider if using PL nanomagnet as a memory element in bit-patterned media or as a generator of magnetic vortices of desired polarity and chirality for microwave applications. Weak interaction among the elements as well as robustness to small external field perturbations makes PL nanomagnet very suitable for operation.

Finally we note, that the sub-100 nm PL nanomagnet is not the only unique design offering control of chirality and polarity by in-plane magnetic field. Qualitatively similar results are obtained in simulations for different sizes and shapes of the missing sector. According to our simple model, the necessary ingredients are symmetry of the object, the demagnetization field strength of removed part and shape anisotropy induced by removed part. Robustness of vortex polarity against B_z is based on vortex - anti-vortex annihilation during vortex core nucleation.

ACKNOWLEDGMENTS

This work has been supported by the project CENTE II, Research & Development Operational Program funded by the ERDF, ITMS 26240120019, and by VEGA 2/0037/12.

* jaroslav.tobik@savba.sk

¹ S.S. Parkin, H. Hayashi, and L. Thomas, *Science* **320**, 190 (2008).

² K.S. Buchanan, P.E. Roy, M. Grimsditch, F.Y. Fradin, K.Yu. Guslienko, S.D. Bader, V. Novosad, *Nat. Phys.* **1**, 172 (2005)

³ C.A. Ross, H.I. Smith, T. Savas, M. Schattenburg, M. Farhoud, M. Hwang, M. Walsh, M.C. Abram, and R.J. Ram, *J. Vac. Sci. Technol.* **B 17**, 3168 (1999).

⁴ S.H. Chung, R.D. McMichael, D.T. Pierce, and J. Unguris, *Phys. Rev. B* **81**, 024410 (2010).

⁵ J.W. Lau and J.M. Shaw, *J. Phys. D* **44**, 303001 (2011).

⁶ R.P. Cowburn, *J. Phys. D* **33**, R1 (2000).

⁷ W.F. Brown, *J. Appl. Phys.* **39**, 993 (1968).

⁸ J. d'Albuquerque e Castro, D. Altbir, J.C. Retamal, and P. Vargas, *Phys. Rev. Lett.* **88**, 237202 (2002).

⁹ M. Schneider, H. Hoffmann, and J. Zweck, *Appl. Phys. Lett.* **79**, 3113 (2001).

¹⁰ T. Taniuchi, M. Oshima, H. Akinaga, and K. Ono, *J. Appl. Phys.* **97**, 10J904 (2005).

¹¹ P. Vavassori, R. Bovolenta, V. Metlushko, and B. Ilic, *J. Appl. Phys.* **99**, 053902 (2006).

¹² M. Jaafar, R. Yanes, D. Perez de Lara, O. Chubykalo-Fesenko, A. Asenjo, E.M. Gonzalez, J.V. Anguita, M. Vazquez, and J.L. Vincent, *Phys. Rev. B* **81**, 054439 (2010).

¹³ K. Yamada, S. Kasai, Y. Nakatani, K. Kobayashi, H. Kohno, A. Thiaville, and T. Ono, *Nature Materials* **6**, 269 (2007).

¹⁴ K.S. Lee, K.Y. Guslienko, J.Y. Lee and S.K. Kim, *Phys. Rev. B* **76**, 174410 (2007).

¹⁵ R. Antos and Y. Otani, *Phys. Rev. B* **80**, 140404 (2009).

¹⁶ V. Cambel and G. Karapetrov, Phys. Rev. B **84**, 014424 (2011).

¹⁷ M.J. Donahue and D.G. Porter, *OOMMF User's Guide, Version 1.0*, Technical Report No. NISTIR 6376, National

Institute of Standards and Technology, Gaithersburg, MD (1999).

¹⁸ To be precise, we mean curvature of field lines projected onto xy plane, since the concept of curvature with sign is meaningful for curves in two dimensions.